

Nonlinear Zeno dynamics due to atomic interactions in Bose-Einstein condensate

V. G. Navarro, V. S. Shchesnovich*

*Centro de Ciências Naturais e Humanas, Universidade Federal do ABC, Santo André, SP,
09210-170 Brazil*

Abstract

We show that nonlinear interactions induce both the Zeno and anti-Zeno effects in the generalised Bose-Josephson model (with the on-site interactions and the second-order tunneling) describing Bose-Einstein condensate in double-well trap subject to particle removal from one of the wells. We find that the on-site interactions induce *only* the Zeno effect, which appears at long evolution times, whereas the second-order tunneling leads to a strong decay of the atomic population at short evolution times, reminiscent of the anti-Zeno effect, and destroys the nonlinear Zeno effect due to the on-site interactions at long times.

Keywords: Zeno effect, Bose-Einstein condensates, Bose-Josephson model

1. Introduction

In a seminal paper Misra and Sudarshan [1] introduced the quantum Zeno paradox by showing that an arbitrary evolution of quantum system comes to a halt due to frequent measurements (for a review, see Ref. [2]). The Zeno slowdown of the quantum evolution (in the decay of an unstable state) was first observed in a two-level system [3]. Since then, understanding of the phenomenon has evolved significantly. It was rederived as a purely dynamical effect (the Zeno effect) without the need for the von Neumann projection postulate [4]. Moreover, besides the slowdown of the evolution of a system (halted decay of an initial quantum state), i.e. the Zeno effect, enhancement of evolution, i.e. the anti-Zeno effect was also discovered [5, 6]. Generally speaking, both effects are demonstration of an external control over the quantum system, as it now understood [7]. There are demonstrations of the Zeno and anti-Zeno dynamical effects in open quantum systems, where both effects observed by varying the frequency of the observation (or the dissipative coupling rate), for instance, in cold sodium atoms [8], in spin-bath models [9], and in nanomechanical resonator

*Corresponding author

Email address: valery@ufabc.edu.br; Tel.: +551149967960/Fax: +551149960090 (V. S. Shchesnovich)

coupled to a point contact [10]. The Zeno effect in a Bose-Einstein condensate (BEC) was first observed experimentally in Ref. [11]. Recently the Zeno-like behavior in a single BEC defect in an optical lattice was recently considered theoretically [12] and observed experimentally [13].

The above Zeno and anti-Zeno effects are due to an *external* influence on the system (i.e. measurements or a thermal bath, etc), however, the dynamical slowdown or enhancement of the system evolution can be also due to internal interactions in the system itself. Such effects are also counterintuitive, for instance, the inhibition of losses due to strong inelastic collisions in cold molecular gases [14]. It was also found that elastic collisions (i.e. ordinary nonlinear interactions) in a bosonic system, namely on-site elastic collisions between the BEC atoms trapped in a double-well potential, lead to visible Zeno-type dynamics [15] which was called the nonlinear Zeno effect. In the latter system the Macroscopic Quantum Self Trapping (MQST) [16, 17] appears simultaneously with the quantum Zeno dynamics, and, in principle, could be responsible for the nonlinear Zeno effect. It is thus of interest to study the respective range of parameters where each of these two effects appears, looking for a domain of the MQST, where the nonlinear Zeno effect does not appear. Moreover, for the same reason, it would be also interesting if one is able to demonstrate the anti-Zeno effect due to nonlinear interactions.

Therefore, we set as the main focus of the present work to study the Zeno dynamics due to two different types of nonlinear interactions. Two different types of interactions are available already in the most general (two-mode) Bose-Josephson model of Ref. [18], describing a BEC in a double-well trap, where there are the on-site interactions in each mode and the second-order tunneling. One of the two modes is subject to an externally controlled particle removal (loss), for instance, due to application of an electron beam to one of the wells, similar as in Refs. [19, 20, 21].

We find that the on-site interactions induce *only* the Zeno effect (at long evolution times), as compared to the non-interacting case. Moreover, we show that there are parameter values for which the MQST effect is expected, but the nonlinear Zeno effect does not appear, which was not addressed in our previous publication [15]. On the other hand, the second-order tunneling modifies the decay dynamics in a way reminiscent of both the anti-Zeno effect at short evolution times and the Zeno effect at intermediate evolution times. Most importantly, the second-order tunneling can completely destroy the nonlinear Zeno effect due to the on-site interactions.

2. Bose-Josephson model with an applied particle removal

The most general two-mode Hamiltonian, describing BEC in an asymmetric double-well potential (i.e. the generalised Bose-Josephson model) was derived in Ref. [18]). It has only two independent parameters describing nonlinear interactions and can be cast as follows (equivalent to the Hamiltonian \hat{H}_2 of Ref. [18])

$$H = -J(a_1^\dagger a_2 + a_2^\dagger a_1) + \beta[(a_1^\dagger a_2)^2 + (a_2^\dagger a_1)^2] + Vn_1 + U(n_2^2 + n_1^2) + 2(\beta - U)n_1 n_2, \quad (1)$$

where a_j and a_j^\dagger ($j = 1, 2$) are the boson operators of the two modes, $n_j = a_j^\dagger a_j$, J is the first-order tunneling rate, V is the zero-point energy bias, U is the local (on-site) nonlinear interaction in each well, and β is second-order tunneling rate. Note that $\beta - U$ is the strength of the nonlinear interactions across the wells of the double well. We set the interaction between the atoms to be repulsive, i.e., $U > 0$, however, the results apply to the attractive case as well, due to a symmetry between the two cases (see, for details, Ref. [22]). We also note that for a BEC in a double-well trap the on-site nonlinear interactions are always stronger than the second-order tunneling (see, for instance, Ref. [18]), i.e., $U > \beta$.

The controlled removal of BEC atoms can be realized, for instance, by using the electron microscopy [23, 24] or by a laser beam. In the former case, a narrow electron beam, ionizing the atoms, is directed to one of the minima of the potential. In both cases, the applied removal is a continuous measurement tool (the actual rate of the condensate decay is directly observed) and can be described in the framework of the standard Markovian approximation [25]. Introducing the removal probability $p \equiv p(k_1, \Delta t)$, where Δt is the time interval and k_m is a population of the m th well, we can write the single atom removal event as a quantum channel [15]:

$$|k_1, k_2\rangle|0\rangle_R \rightarrow \sqrt{p}|k_1 - 1, k_2\rangle|1\rangle_R + \sqrt{1 - p}|k_1, k_2\rangle|0\rangle_R, \quad (2)$$

where the atoms are removed from well 1, $|k_1, k_2\rangle = \frac{(a_1^\dagger)^{k_1} (a_2^\dagger)^{k_2}}{\sqrt{k_1! k_2!}}|0\rangle$ is the ket-vector of the BEC state and $|j\rangle_R$ describes the atom counter. For the atom removal rate Γ and a small Δt we get $p(k_1, \Delta t) \approx \Gamma k_1 \Delta t$, where Δt is much less than the characteristic first-order tunneling time, defined as $t_{QT} = \hbar/J$.

Introducing the reduced density matrix ρ of the BEC alone, the quantum channel (2) can be described, for small times, by the Kraus superoperator representation $\rho \rightarrow M_0 \rho M_0^\dagger + M_1 \rho M_1^\dagger$, where for a small Δt we have $M_0 \approx 1 - \Gamma n_1 \Delta t / 2$ and $M_1 \approx \sqrt{\Gamma \Delta t} a_1$. This leads to the master equation in the Lindblad form

$$\frac{d\rho}{dt} = -\frac{i}{\hbar}[H, \rho] + \Gamma \left\{ a_1 \rho a_1^\dagger - \frac{n_1}{2} \rho - \rho \frac{n_1}{2} \right\}. \quad (3)$$

The operator $\mathcal{D}(\cdot) = a(\cdot)a_1^\dagger - \{n_1, (\cdot)\}/2$ has only negative eigenvalues $\lambda \in \{-N, -N + 1/2, \dots, -1/2, 0\}$, where N is the total number of atoms, i.e. the only stationary state of the operator \mathcal{D} is $\rho_0 = |0\rangle\langle 0|$.

The case of interacting bosons can be compared to the non-interacting case, where the exact solution is readily available [15]. Indeed, for $U = \beta = 0$, setting also $V = 0$, for simplicity, and assuming that initially the condensate is in the

ground state $|\psi\rangle = \frac{(a_1^\dagger + a_2^\dagger)^{N_0}}{\sqrt{2^{N_0} N_0!}} |0\rangle$ one can derive the explicit solution [15]

$$\langle N \rangle = e^{-\frac{\Gamma}{2}t} \left[\frac{J^2}{(\hbar\Omega)^2} - \frac{\Gamma^2}{16\Omega^2} \cos(2\Omega t) \right] N_0, \quad (4)$$

$$\langle n_1 - n_2 \rangle = -e^{-\frac{\Gamma}{2}t} \frac{\Gamma}{4\Omega} \sin(2\Omega t) N_0, \quad (5)$$

where $\Omega = \sqrt{\frac{J^2}{\hbar^2} - \frac{\Gamma^2}{16}}$. Let us briefly recall how the Zeno effect appears in the Bose-Josephson model [15]. When $\Gamma < 4J/\hbar$, Eqs. (4) and (5) describe the decaying Rabi oscillations with the decay rate $\Gamma/2$. For $\Gamma \gg 4J/\hbar$, the dynamics is characterized by two different loss rates: the initial stage with the rate $\Gamma/2$ and, for times exceeding $1/\Gamma$, a dramatically reduced dissipation rate $\Gamma_{QT} \approx \frac{4J^2}{\hbar^2\Gamma}$. The inverse dependence of the actual loss rate on a strong dissipation is the essence of the Zeno effect. By introducing the tunneling frequency $\omega_R = 2J/\hbar$ one obtains the following expression for the actual decay rate $\Gamma_{QT} = \omega_R^2/\Gamma$. We note that in the latter form our decay rate is equivalent to that observed in the continuous Zeno effect of Ref. [11].

Below we will use the following dimensionless control parameters: the normalized applied rate $\gamma = \Gamma t_{QT} = \Gamma\hbar/J$, the nonlinear on-site interactions strength $\Lambda = UN_0/(2J)$, the energy bias $\varepsilon = V/J$, and the second-order tunneling rate $\delta = \beta N_0/(2J)$, where N_0 is the initial number of atoms.

3. Mean-field approximation

We find that in the limit of a large number of atoms $N \gg 1$ one can use the mean-field approximation obtained by decoupling the averages as follows (see also Ref. [15]): $\langle n_j a_j^\dagger a_{j''} \rangle \approx \langle n_j \rangle \langle a_j^\dagger a_{j''} \rangle$. We have the following mean-field variables z , ϕ , and q , which correspond to the quantum averages:

$$z = \frac{\langle n_1 \rangle - \langle n_2 \rangle}{\langle n_1 \rangle + \langle n_2 \rangle}, \quad q = \frac{\langle n_1 \rangle + \langle n_2 \rangle}{N_0}, \quad e^{i\phi} = \frac{\langle a_1^\dagger a_2 \rangle}{\sqrt{\langle n_1 \rangle \langle n_2 \rangle}}. \quad (6)$$

The mean-field equations read (with $\tau = t/t_{QT} = Jt/\hbar$)

$$\frac{dz}{d\tau} = -2\sqrt{1-z^2} \sin \phi - \frac{\gamma}{2}(1-z^2) + 4\delta(1-z^2)q \sin(2\phi), \quad (7)$$

$$\frac{d\phi}{d\tau} = \frac{2z}{\sqrt{1-z^2}} \cos \phi + \varepsilon + 2(\Lambda - 2\delta)zq - 4\delta zq \cos(2\phi), \quad (8)$$

$$\frac{dq}{d\tau} = -\frac{\gamma}{2}q(1+z). \quad (9)$$

The system of Eqs. (7)-(9) reduces to the mean-field equations of Ref. [15] when $\delta = 0$. For $\gamma = 0$ (and, hence, $q = 1$) the system coincides with the mean-field

system of Ref. [18] and is Hamiltonian, i.e., $\dot{z} = -\frac{\partial \mathcal{H}}{\partial \phi}$ and $\dot{\phi} = \frac{\partial \mathcal{H}}{\partial z}$ with the Hamiltonian

$$\mathcal{H} = (\Lambda - 2\delta)z^2 + \varepsilon z - 2\sqrt{1 - z^2} \cos \phi + 2\delta(1 - z^2) \cos(2\phi). \quad (10)$$

We have verified that the numerical solutions obtained by the Monte Carlo method (a.k.a. the quantum jumps method) [26] are well approximated by the mean-field Eqs. (7)-(9), where the Monte Carlo simulations were certified by comparison with the exact solution (4) in the linear case. We have found that there is a good agreement of the mean-field dynamics with the exact quantum dynamics already for $N \gtrsim 10$. Therefore, below we use the mean-field Eqs. (7)-(9) since they allow to significantly reduce the computation time (and that they are an excellent approximation for $N \gtrsim 100$).

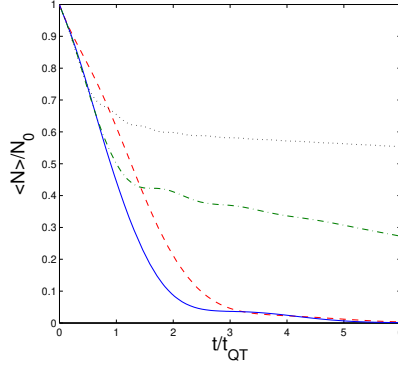


Figure 1: The average ratio of the number of particles in the system. Here $\gamma = 2$, and $\varepsilon = \delta = 0$. We show the results of the numerical simulations for $\Lambda = 0$ (the solid line), $\Lambda = 5$ (the dashed line), $\Lambda = 7$ (the dash-dotted line) $\Lambda = 10$ (the dotted line).

4. Numerical simulations

We first study the nonlinear Zeno effect due to the on-site interactions, first discovered in Ref. [15], by setting $\delta = 0$ and $\varepsilon = 0$ (for simplicity). The results are presented in Fig. 1. Observe that at short times the interactions leave the behavior of the linear (non-interacting) case (4) visibly unmodified, whereas at long times the Zeno effect is clearly observed in comparison to the linear case for $\Lambda = 7$, for times $t \gtrsim 2t_{QT}$, and for $\Lambda = 10$, for times $t \gtrsim 1.5t_{QT}$. At all values of the on-site interaction strength greater than the critical $\Lambda_{cr} = 1$ there is the MQST state in the closed system, i.e. for $\gamma = 0$ [17, 22]. On the other hand, the Zeno effect appears for larger $\Lambda > 5$, since at $\Lambda = 5$ the average number of particles also reduces to zero (whereas if the MQST were responsible for the effect, it should have been finite). One thus concludes that the MQST is not the mechanism responsible for the remaining finite fraction of the particles in the

system for $\Lambda = 7$ and $\Lambda = 10$ in Fig. 1. Hence, the latter effect can be rightfully called the nonlinear Zeno effect, which confirms the main conclusion of Ref. [15].

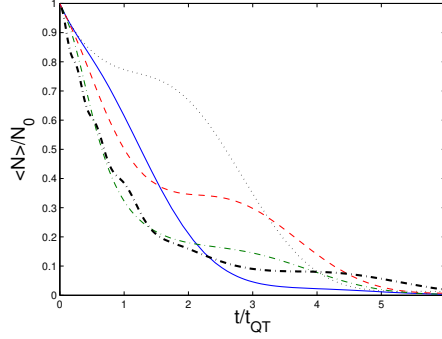


Figure 2: The average ratio of the number of particles in the system. Here $\gamma = 2$, and $\varepsilon = \Lambda = 0$. We show the results of the numerical simulations for $\delta = 0$ (the solid line), $\delta = 1$ (the dotted line), $\delta = 2$ (the dashed line), $\delta = 3$ (the dash-dotted line), and $\delta = 10$ (the tick dash-dotted line).

The influence of the second-order tunneling on the actual decay rate in the system is richer than that of the on-site interactions. To elucidate its influence, we consider first the second-order tunneling alone by setting $\Lambda = 0$ (and $\varepsilon = 0$ for simplicity). The results are presented in Fig. 2. It is seen that the second-order tunneling can result in both the Zeno and anti-Zeno effects, where the anti-Zeno effect appears for $\delta \geq 2$ at short evolution times, whereas the Zeno effect appears at intermediate evolution times. Specifically, for $\delta = 1$ we see no anti-Zeno effect, whereas a visible Zeno effect appears in the time window $t_{QT} \lesssim t \lesssim 2t_{QT}$ for $\delta = 1$, in the time window $1.5t_{QT} \lesssim t \lesssim 3t_{QT}$ for $\delta = 2$ and $\delta = 3$, and in the time window $2t_{QT} \lesssim t \lesssim 5t_{QT}$ for $\delta = 10$. However, it is seen that the Zeno dynamics due to the second-order tunneling is transient, since for long times the decay is comparable to that of the linear case.

Finally, we study the effect of the combined action of the on-site interactions and the second-order tunneling. The results are presented in Fig. 3. We see that the second-order tunneling destroys the nonlinear Zeno effect due to the on-site interactions. Moreover, there is a visible anti-Zeno dynamics due to the combined action of the second-order tunneling and the on-site interactions (for instance, for $\Lambda = 10$ and $\delta \geq 1.5$). By examining the mean-field Eqs. (7)-(9) one can see that the second-order tunneling has two contributions: it induces an effective zero-point energy bias between the modes similar as the on-site interactions term, where the effective bias due to the nonlinear interactions is $\varepsilon_{NL} = 2(\Lambda - 2\delta)qz$. We note that for $\delta = 0$ the latter effective energy bias

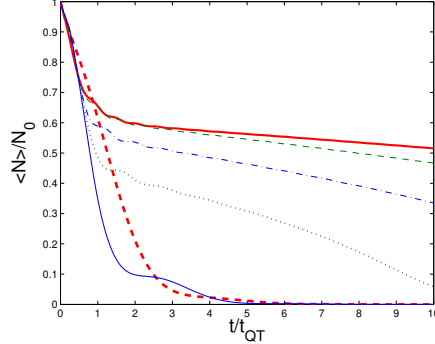


Figure 3: The average ratio of the number of particles in the system. Here $\gamma = 2$, and $\varepsilon = 0$. We show the results of the numerical simulations for $\Lambda = 10$ and various values of δ , with $\delta = 0$ (the thick solid line), $\delta = 1$ (the thin dashed line), $\delta = 1.5$ (the dot-dashed line), $\delta = 1.7$ (the dotted line), and $\delta = 2$ (the thin solid line) in comparison with $\Lambda = \delta = 0$ (the thick dashed line).

explains the decay rate due to the nonlinear Zeno effect derived in Ref. [15],

$$\Gamma_{NL} \approx \frac{4\Gamma}{\gamma^2 + 4\varepsilon_{NL}^2}, \quad (11)$$

which was shown to be an excellent approximation to the observed decay rate for $t \gtrsim 1/\Gamma$ provided that $\gamma^2 + 4\varepsilon_{NL}^2 \gg 1$ [15]. Thus one would expect that for $\delta \neq 0$ the second-order tunneling would also contribute to the Zeno effect. However, the second-order tunneling has also the pair tunneling term which in the mean-field system (7)-(9) is given by the last terms in Eqs. (8) and (9) (with the $\cos(2\phi)$ and $\sin(2\phi)$). We thus have found that this contribution dominates, leading to the destruction of the Zeno effect due to the nonlinear interactions, resulting in a rapid decay of the atomic population comparable or faster than that of the linear (i.e. non-interacting) case.

Here we note that a sufficiently strong second-order tunneling, due to contribution to on-site interactions term, was previously found to modify the phase transition from the Mott insulator phase to the superfluid phase in the generalized Bose-Hubbard model. Indeed, it induces a new phase transition from a Mott insulator with one particle per site to a superfluid of spatially extended particle pairs living on top of the Mott background, instead of the usual transition to a superfluid of single particles/holes [27].

5. Conclusion

We have studied the Zeno dynamics due to two types of nonlinear interactions in the Bose-Josephson model, the on-site particle scattering and the

second-order, i.e. pair, tunneling. We have found that the on-site interactions induce only the nonlinear Zeno effect at long evolution times, which has a larger threshold value of the interaction parameter than the Macroscopic Quantum Self-trapping. On the other hand, the second-order tunneling is found to induce both the anti-Zeno effect at short evolution times and the Zeno effect at intermediate times. The latter effect is transient, since at long evolution times the atomic decay is similar to the linear case without nonlinear interactions.

Most importantly, we have found that the second-order tunneling can lead to complete destruction of the Zeno effect due to the on-site interactions at long times leading to a strong decay of the atomic population, comparable or stronger than in the non-interacting case. This effect occurs even when there are strong on-site interactions for the second-order tunneling rate comparable to that of the linear tunneling in the system. The anti-Zeno effect thus is a signature of the second-order tunneling in the Bose-Einstein condensate trapped in a double-well potential.

6. Acknowledgements

The authors acknowledge the financial support by the CNPq and CAPES of Brazil.

References

- [1] B. Misra and E. C. G. Sudarshan, J. Math. Phys. **18**, 756 (1977).
- [2] P. Facchi and S. Pascazio, J. Phys. A: Math. Theor. **41**, 493001 (2008).
- [3] W. M. Itano, D. J. Heinzen, J. J. Bollinger, and D. J. Wineland, Phys. Rev. A **41**, 2295 (1990).
- [4] S. Pascazio and M. Namiki, Phys. Rev. A **50**, 4582 (1994).
- [5] A. G. Kofman and G. Kurizki, Nature **405**, 546 (2000).
- [6] A. P. Balachandran and S. M. Roy, Phys. Rev. Lett. **84**, 4019 (2000).
- [7] A. G. Kofman and G. Kurizki, Phys. Rev. Lett. **87**, 270405 (2001).
- [8] M. C. Fischer, B. Gutiérrez-Medina, and M. G. Raizen, Phys. Rev. Lett. **87**, 040402 (2001).
- [9] D. Segal and D. R. Reichman, Phys. Rev. A **76**, 012109 (2007).
- [10] P. W. Chen, D. B. Tsai, and P. Bennett, Phys. Rev. B **81**, 115307 (2010).
- [11] E. W. Streed, J. Mun, M. Boyd, G. K. Campbell, P. Medley, W. Ketterle, and D. E. Pritchard, Phys. Rev. Lett. **97**, 260402 (2006).
- [12] D. A. Zezyulin, V. V. Konotop, G. Barontini, and H. Ott, Phys. Rev. Lett. **109**, 020405 (2012).

- [13] G. Barontini, R. Labouvie, F. Stubenrauch, A. Vogler, V. Guarrera, and H. Ott, Phys. Rev. Lett. **110**, 035302 (2013).
- [14] N. Syassen *et al*, Science **320**, 1329 (2008).
- [15] V. S. Shchesnovich and V. V. Konotop, Phys. Rev. A **81**, 053611 (2010).
- [16] L. Bernstein, J. C. Eilbeck and A. C. Scott, Nonlinearity **3**, 293 (1990).
- [17] A. Smerzi, S. Fantoni, S. Giovanazzi, and S. R. Shenoy, Phys. Rev. Lett. **79**, 4950 (1997); S. Raghavan, A. Smerzi, S. Fantoni, and S. R. Shenoy, Phys. Rev. A **59**, 620 (1999).
- [18] D. Ananikian and T. Bergeman, Phys. Rev. A **73**, 013604 (2006).
- [19] T. Gericke, C. Utfeld, N. Hommerstad, and H. Ott, Las. Phys. Lett. **3**, 415 (2006).
- [20] T. Gericke, P. Würtz, D. Reitz, T. Langen, and H. Ott, Nat. Phys. **4**, 949 (2008).
- [21] V. A. Brazhnyi, V. V. Konotop, V. M. Pérez-García, and H. Ott, Phys. Rev. Lett. **102**, 144101 (2009).
- [22] V. S. Shchesnovich and M. Trippenbach, Phys. Rev. A **78**, 023611 (2008).
- [23] T. Gericke, C. Utfeld, N. Hommerstad and H. Ott, Las. Phys. Lett. **3**, 415 (2006).
- [24] T. Gericke, P. Würtz, D. Reitz, T. Langen and H. Ott, Nature Phys. **4**, 949 (2008).
- [25] H. P. Breuer and F. Petruccione, *The Theory of Open Quantum Systems* (Oxford University Press, Oxford, 2002).
- [26] K. Mølmer, Y. Castin and J. Dalibard, J. Opt. Soc. Am. B **10**, 524 (1992); H. Carmichael, *An Open Systems Approach to Quantum Optics* (Springer, Berlin, 1993).
- [27] O. Dutta, A. Eckardt, P. Hauke, B. Malomed, and M. Lewenstein, New J. Phys. **13**, 023019 (2011).